APEM journal
Advances in Production Engineering & Management
Volume 19 | Number 4 | December 2024 | pp 443–459
https://doi.org/10.14743/apem2024.4.518
ISSN 1854-6250
Journal home: apem-journal.org
Original scientific paper

Optimizing electric vehicle charging strategies using multi-layer perception-based spatio-temporal prediction of charging station load

Wang, Y.N.[a], **Zhang, Z.J.**[a], **Ping, A.**[a,*], **Wang, R.J.**[a], **Gong, D.Q.**[a]

[a]School of Economics and Management, Beijing Jiaotong University, Beijing, P.R. China

ABSTRACT

The production and sales of electric vehicles have been increasing in line with the gradual adaptation of consumers to electric vehicles, driven by various government policies and subsidies over the past decade. As a result, the deployment of charging facilities, which are essential for supporting electric vehicles, has also been extensive. However, despite the rapid development in scale, charging facilities face challenges such as low utilization during off-peak hours and excessive congestion during peak hours, leading to resource wastage and a diminished user charging experience. To address these issues, this study proposes a spatio-temporal prediction model for charging station load. The model introduces a global spatial enhancement module to simultaneously learn short-range and long-range spatial dependencies in the data, resulting in improved prediction accuracy. The aim of this research is to provide practical guidance in terms of conserving charging resources and enhancing user charging experience based on spatio-temporal prediction effectiveness.

ARTICLE INFO

Keywords:
Electric vehicles;
Spatio-temporal prediction;
Charging station load;
Multi-layer perception (MLP)

**Corresponding author:*
23111184@bjtu.edu.cn
(Ping, A.)

Article history:
Received 6 August 2024
Revised 5 December 2024
Accepted 12 December 2024

1. Introduction

With the increasing awareness of environmental protection and the increasing preciousness of fossil energy, Electric Vehicle (EV) has gradually become a key to address the issues of environmental pollution and energy shortage due to its clean and low-carbon features [1]. Hence, it is evident that the electric vehicle industry has garnered substantial attention and support worldwide. Numerous governments have implemented a range of policy measures to facilitate the development of electric vehicles. The Chinese government, in particular, has demonstrated a high level of commitment to the electric vehicle industry. In recent years, the National Development and Reform Commission, the Ministry of Finance, the Ministry of Industry and Information Technology, and other relevant departments have jointly issued the Notice on Financial Subsidies for the Promotion and Application of New Energy Vehicles (Caijian [2020] No. 86) [2]. With incentives such as financial subsidies, tax incentives and quotas for vehicle purchase targets, the production and sales of electric vehicles have continued to rise in the domestic market. According to the China Association of Automobile Manufacturers (CAAM), the production and sales of new energy vehicles in 2022 were completed at 7,058,000 and 6,887,000 units, respectively, representing year-

on-year growth of 96.9 % and 93.4 %. In the development plan for the future, the Energy Saving and New Energy Technology Roadmap of the China Society of Automotive Engineering expects that by 2025, China's new energy vehicle production and sales will reach 8 million units. In the next five years, the market size of new energy vehicles will grow even more rapidly and is expected to reach 15 million units by 2030 [3]. In addition, the promotion of electric vehicles is a key initiative to promote the development of green transformation in the global power and transportation sectors, and to achieve the strategic goals of carbon peaking and carbon neutrality (dual-carbon), and the Paris Agreement has set a target of 100 million electric vehicles in the world by 2030. This indicates that the number of electric vehicles worldwide has exploded in recent years and will continue to grow in the coming years.

Therefore, electric vehicle charging infrastructure, which is the energy supply for electric vehicles, will develop rapidly under the trend of growth in the number of electric vehicles. To meet the increasingly diverse charging demands of electric vehicle drivers, governments and enterprises at all stages have invested in the construction of charging piles, charging stations and other facilities. However, some issues need to be resolved while the number and scale of charging facilities are expanding. First, 'no pile for vehicles, no vehicle for piles' means that the layout and distribution of electric vehicle charging facilities are not reasonable enough, and the situation has gradually revealed itself. In some regions, the supply of charging piles at charging stations is well below the demand of electric vehicles, and the symptom of charging difficulty has appeared [4]. Simultaneously, in other regions, charging stations are overbuilt with a large number of charging piles lying idle, which is a severe waste of resources. This situation reflects the mismatch between the construction of charging facilities and EV ownership. Moreover, the generally low utilization rate of charging infrastructure is accompanied by the phenomenon of peak congestion. Due to the uneven distribution of charging facilities and the volatility of EV users' charging demand, there are obvious peaks and troughs in the utilization of many charging facilities. Underutilization not only wastes resources, but also reduces the experience of EV users during peak congestion, which in turn affects the acceptance of EVs in the EV consumption market. This study finds that the centrepiece of the above issues is the result of the uneven spatial and temporal spread of EV charging station loads that is specifically evident [5].

A possible solution is to analyse the spatial and temporal distribution patterns of loads at EV charging stations and use them as a basis for predicting the spatial and temporal distribution of loads [6]. The main contributions of this study are summarized as follows:

- We built the model structure with higher prediction performance for loaded spatio-temporal data.
- In the spatio-temporal prediction model, we innovatively built a global spatial enhancement module, which enables the model to learn global spatial information directly. Compared with the traditional convolutional learning method that gradually improves the sensory field by stacking, the global spatial reinforcement module improves the model's learning effect on the spatial-dependent features of charging station loading over long distances.
- In terms of prediction model accuracy, the model we built is better than the baseline model in comparison tests, as quantified by two evaluation metrics, with 10.2 % and 7.3 % improvement, respectively.

2. Literature review

2.1 Charging selection behaviour

The charging choice behaviour of electric vehicle users is quite different from the traditional refuelling behaviour of fuel vehicle users. Therefore, the study of EV users' charging choice behaviour has begun to receive extensive attention from both the academic and technical communities. Li *et al.* revealed that range uncertainty has a significant impact on users' charging behaviour [7]. When the range uncertainty is high, users will have a greater tendency to charge their EVs when the remaining power is high, in order to reduce the contingencies caused by insufficient power.

Therefore, its subsequent study proposed an ordered probability distribution model and suggested that the availability of charging facilities, distance and charging time are important influences on users' charging behaviour [8]. Meanwhile, Yang *et al.* studied charging behaviour selection optimization by using a bi-level optimization model and found that EV drivers are influenced by a variety of factors in charging and route selection, including charging facility availability, distance, charging time, and charging price, etc. [9]. Latinopoulos and Sivakumar found that there is also a close relationship between charging location, driving distance, and range anxiety. The above studies reveal that the charging choice behaviour of EV users is influenced by a variety of factors including availability of charging facilities, distance, charging time, price, remaining charge [10], and battery range.

2.2 Charging station load capacity and influencing factor

The load of charging station comes from the selection and interaction behaviour of users with charging station, so the charging selection behaviour of users influences the distribution and change rule of charging station load. Al-Kandari and Soliman in 2003 proposed a load prediction model that integrates the consideration of multi-source information and the adjustment of users' decision-making, and the study considered the influence of users' behavioural patterns and decision-making strategies on the prediction effect [11]. Sani's team also conducted a study on the robust integration of electric vehicle charging loads in smart grid capacity expansion planning [12], to improve the robustness and reliability of grid operation. The study focuses on the impact of user behaviour on the planning and integration process, where user behaviour includes uncertainty in charging demand, user's charging time period selection, and fluctuation in charging behaviour.

The EV charging station load in this study is defined as the number of charging piles working at a charging station at a given point in time is equal to the number of EVs undergoing charging operations. If the number of EVs in a charging station is close to or equal to the maximum charging load limit of the current charging station, queuing and congestion occurs at that charging station, i.e., the charging station is overloaded. If the number of EVs being charged is significantly less than the maximum charging position limit of the current charging station, this represents a more relaxed idle state of the current charging station. Therefore, the influencing factors affecting the charging station load and its spatio-temporal distribution is a relatively complex dynamic problem [13].

First, regarding the charging price factor, two scholars proposed a data-driven approach based on using conditional random field modelling in order to perform a spatio-temporal price elasticity analysis of public charging demand for EVs [14]. Meanwhile, Wang *et al.* proposed an integer hybrid planning model in which a vehicle-to-grid (V2G) model is implemented by analysing spatio-temporal electricity prices and grid load profiles, which integrates electric vehicles into the grid for energy delivery and exchange through battery swapping, thus acting as a peak-shaving and valley-filling agent for electricity [15]. Second, geographic factors: The location of charging stations and the characteristics of the surrounding environment are also an important factor affecting the spatial and temporal distribution of charging station loads. Both factors can affect the utilization rate and charging capacity of charging stations. Bian found that the planning of EV fast charging stations should be based on point-of-interest segmentation, functional zones, and multiple spatio-temporal features [16]. Points of interest (POIs) help identify potential charging needs, functional zones enhance services and functions for charging stations, and multiple spatio-temporal features further optimize the planning and layout of charging stations. Zhang *et al.* proposed an EV charging demand prediction method considering the fine division of functional zones based on the characteristics of the functional zones of the city, which are divided into different functional zones, such as residential, commercial, and industrial zones [17].

The time factor is a key influence on charging station loads, with effects from factors such as morning and evening peak hours, weekends, holidays, and seasons impacting the spatial and temporal distribution of charging station loads. Bayram and Galloway focused on pricing strategies and distributed control for fast EV charging stations operating in cold climates [18]. Research has shown that cold weather can affect battery performance, leading to reduced charging efficiency, increased charging time, and influencing user charging behaviour decisions to some extent. Louie

modelled the time series of EV charging station loads. By analysing the data of EV charging station loads, it was found by Louis that the loads exhibit distinct time series characteristics, including random fluctuations, multiple periodicities, and long-term trends [19]. Additionally, Bampos *et al.* developed a predictive model for the electric vehicle load curve (EVLC) [20]. Seasonal variations in the predicted performance are explored, deepening the importance of the impact of seasonal characteristics on research in this field.

Spatial factors also play a role in influencing charging station loads. This is because the loads between adjacent charging stations may affect each other, depending on factors such as their distance, number, capacity, type, usage patterns, and demand. In areas with high charging station density, stations may compete with each other, leading to uneven loads. Conversely, in more dispersed layouts, users may consider additional factors when selecting a station, reducing mutual impact. Huang and Kockelman developed a network equilibrium model and considered the elasticity of demand for EV charging and congestion at charging stations [21]. It was found that the location selection of charging stations should consider the spatial and temporal distribution of EV charging demand, the congestion of charging stations, and the interaction between charging stations. In particular, an excessive number of charging stations on a regional scale can lead to intense competition between charging stations and network congestion, thus reducing the efficiency of the entire charging network.

The travel demand and charging demand of EV users can also be affected by special circumstances such as holiday periods and participation in large events. Unterluggauer proposed a short-term load prediction model for EV charging stations using a multivariate multi-step short-term memory approach [22]. The effect of holidays was used as one of the input variables of the model in the study, this is because the researcher found that holidays may have a significant effect on the load of EV charging stations. For example, during holidays, people's travel patterns and charging needs may be very different from normal working days, which may lead to results such as higher load fluctuations at charging stations.

3. Research methodology

3.1 Multi-source data

In this study, the data types of multi-source dataset are used to cover the business data of EV users' charging behaviours at charging stations in Shanghai, the equipment information data of EV charging stations, the POI basic information data, the weather data, holidays, and other environmental data. Table 1 shows a brief introduction of the data names and contents.

The total amount of data on charging behaviour at charging stations for the period of August 30, 2020 to February 28, 2021 for the specific data involved in this study is approximately 117.6 million. The total number of data items is 64 columns. The number of data pieces totals 1,095,889. By processing the business data and equipment data of charging stations, based on the latitude and longitude location of the charging stations, we get the specific allocation of the relevant charging stations shown in Fig. 1.

Table 1 Detailed introduction of data source and data content

Data name	Data content	Data source
Operational data	Operational data generated by users during charging	Shanghai charging station online platform
Charging station facility data	Charging station facility information and geographic location	Shanghai charging station online platform
Road network data	Shanghai's road location and road property	OpenStreetMap open-source dataset
Points of interest data	POI name, type and geographic location	Gaode Map API
Weather data	Temperature, precipitation, wind, etc. of the day	National meteorological data sharing platform
Holiday data	The dates of national legal holidays	State council website announcement

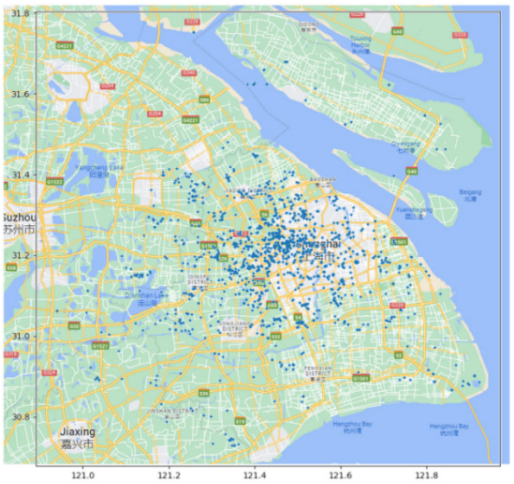

Fig. 1 Distribution diagram of charging station

Fig. 2 Visualization of Shanghai road network data classification

Meanwhile, by using the Shanghai road network data from the OpenStreetMap open source road information database, we simplified the road types in the data structure of the open source database for the convenience of the study. First, according to the *TYPE-Road Type* attribute, *highway* and *urban expressway* are grouped into *A* and *B* road types, which represent the roads that need to be connected to the road network *A*, which represents the type of road that requires the user to drive faster across the spatial distance per unit of time. Second, *urban main roads* and *urban secondary roads* are grouped together as *B* roads, which represent a road type that requires users to cross a moderate distance per unit of time while driving. Finally, *urban branch roads* and *rural roads* are categorized as *C* roads, which represent a type of road that crosses a slower distance per unit of time when the user is driving. The road network visualization of the above three road types is shown in Fig. 2.

3.2 Time distribution characteristics

The patterns of change in charging station loadings in the time dimension include short-term patterns of change, multiple periodicities, long-term trends, and the effects of special events.

Fig. 3 shows the short time variation of the load of the charging station. The results indicate that the load at a specific time of day is influenced by the load values from the preceding neighbouring hours. Analysing the daily load trend reveals a consistent pattern, characterized by gentle upward and downward fluctuations.

Figs. 4 and 5 show the multiple periodicities characterising the variation of the charging station load values. Multiple periodicity refers to the presence of several cycles with different lengths in the load values. The charging station loads at a specific time are influenced by loads spanning

multiple previous cycles. The periodic effects observed include the same hour of previous days as well as the same hour of the corresponding days from previous weeks, which affect the charging station load at the target time. This pattern is derived from the results of the autocorrelation function method.

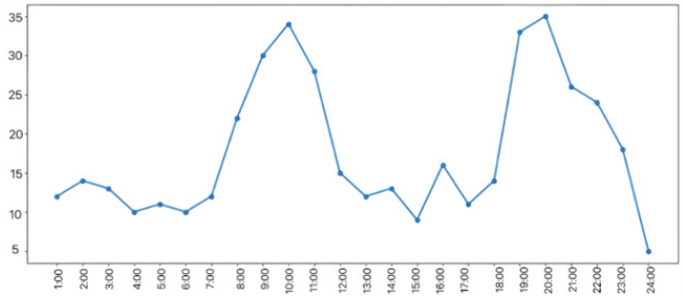

Fig. 3 Diagram of daily charging load variation at a charging station in Shanghai

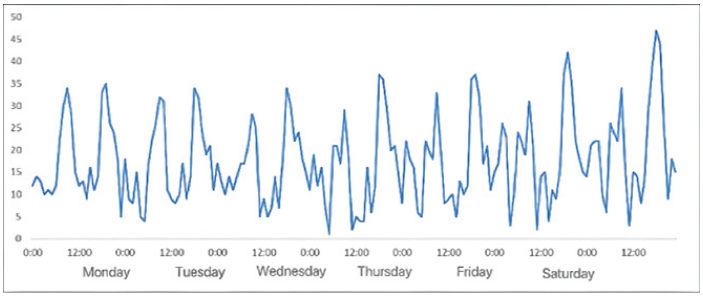

Fig. 4 Change in load capacity of charging station within one week

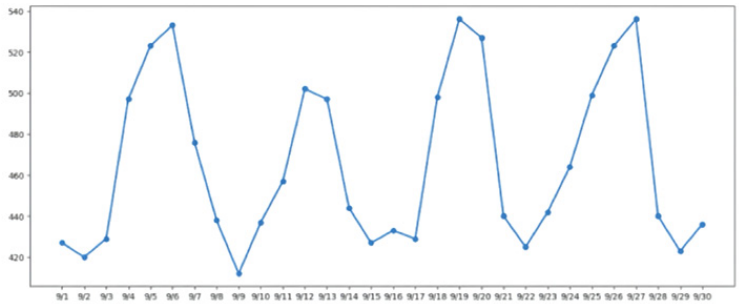

Fig. 5 Loading capacity of charging station varies continuously for multiple weeks

As shown in Fig. 6, this represents a long-term trend in the values of charging station loads. By changing through time, the charging station loads will have an overall trend of increasing in fluctuation. This regularity is reflected according to the results of the exponential smoothing method.

The pattern of change in the value of the charging station load is affected by some special effects, including legal holidays (Fig. 7) and special weather such as rainy and snowy days. This feature is analysed by multiple linear regression method.

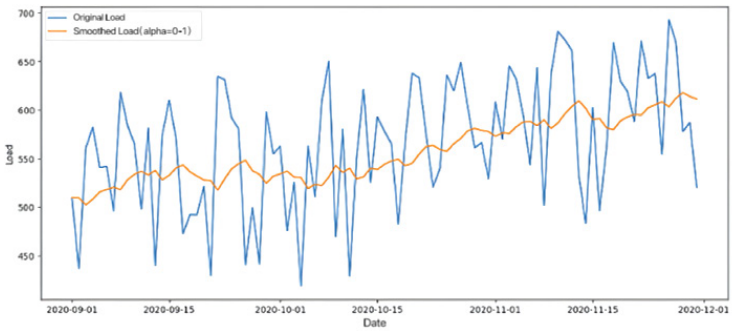

Fig. 6 Smoothing result of charging station load index

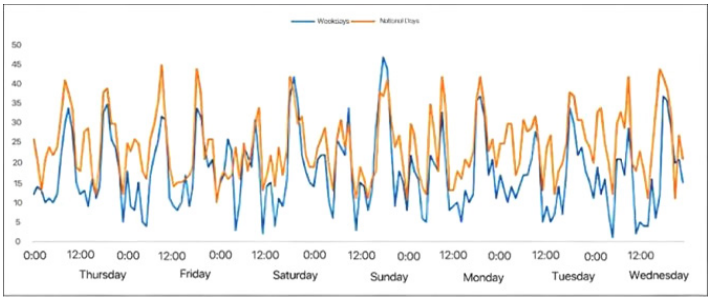

Fig. 7 Trend of load changes during the National Day holiday(seven-day time period)

Despite holidays, weather should also be considered as a factor that affects the time series trend of charging station loads. This is because special weather, such as rain, fog, and snow, can affect the travel decisions and charging decisions of electric vehicle users. Similar to the method of observing the effect of legal holiday factors on the time series of charging station loads, the study compares the trends of the hourly granularity of loads within an average single day under four types of weather, namely, rainy day, snowy day, foggy day, and normal. It is found that the charging station loads in rainy, snowy, and foggy days are overall smaller than the charging station loads under normal days in all hours. This study attempts to find a linear function such that the dependent variable can be explained by a weighted combination of the independent variables.

In this case, Y is the dependent variable, X_1 to X_k are independent variables, β_0 is the intercept, β_1 to β_k are the regression coefficients, and ε is the error term.

$$Y = \beta_0 + \beta_1 X_1 + \beta_2 X_2 + \cdots + \beta_k X_k + \varepsilon \quad (1)$$

The study in this paper uses four dummy variables to represent weather conditions (holiday, rain, snow, and fog). Each dummy variable is a binary indicator variable that takes the value of 0 or 1. Such variables can help in understanding the effect of different weather conditions on loadings. Thereafter, least squares regression was used and statistical information such as estimates of regression coefficients, t-statistics, and p-values were obtained. This information helps to understand the relationship between the independent and dependent variables. For example, the regression coefficient indicates the amount of change expected in the dependent variable when the independent variable is increased by one unit. The p-value helps to determine whether the relationship is significant or not. In the data of this paper, it was found that holidays have a significant positive effect on loadings at the $p < 0.01$ level, while rainy and snowy days have a negative effect on loadings at the $p < 0.05$ level, and foggy days have a non-significant effect on loadings, as detailed in the analyses shown in Table 2.

Table 2 Multiple linear regression results with special time effects

Special time	Coefficient	t value	p value
Legal holidays	14.25	7.476	0.004**
Rainy days	-3.49	-1.828	0.039*
Snowy days	-6.52	-3.417	0.045*
Foggy days	-4.50	-2.361	0.077

3.3 Spatial distribution characteristics

This study defines charging stations with straight line distance between charging stations within 3 km and road form distance within 5 km as relatively close charging stations. Others are defined as relatively distant charging stations. There are three patterns of influence of charging station loads in the spatial dimension. Firstly, a charging station with saturated charging load will transmit the excess charging demand in the area to the close charging station. This means that when a charging station reaches saturation charging load, it will transfer a portion of the load to neighbouring charging stations, causing the loads of the neighbouring charging stations to rise This phenomenon is particularly common during peak periods. As well, there is competition between neighbouring charging stations that have not yet saturated their loads. Because they need to share limited resources, if the load of a charging station that has not yet saturated increases, it will affect

the load of neighbouring charging stations, as shown in Fig. 8. Secondly, high-load charging stations near points of special interest, such as commercial centres, tend to cluster. This is because charging stations located near commercial centres attract more electric vehicles (EVs), leading to an increase in charging demand at multiple stations in the surrounding area.

In this study, the effect of point-of-interest factors on EV mobility patterns and charging load distribution is considered. Charging stations within 2 km from the point of interest are defined as charging stations around the point of interest. Using multiple linear regression and least squares method, the study quantitatively assesses the degree of influence and the confidence level of different types of points of interest on charging station loads. The details are shown in Table 3, where the coefficients represent the degree and direction of the influence of the point of interest feature on the load of the surrounding charging stations, and the *p*-value represents the confidence level of whether an influence exists. $p < 0.05$ means that there is a confidence in the influence of the corresponding point of interest feature, and $p < 0.01$ represents a higher level of confidence.

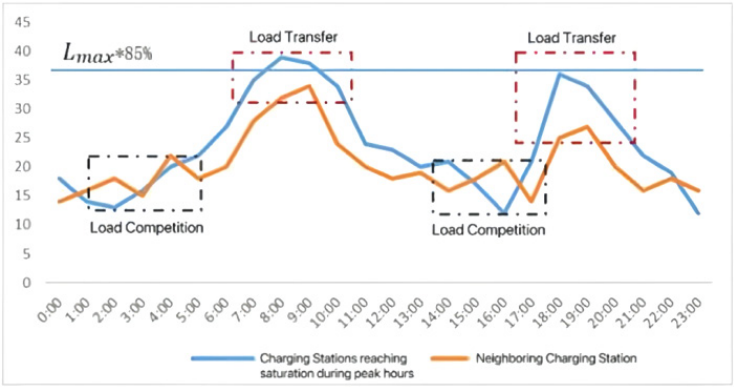

Fig. 8 Influence of saturated charging stations on adjacent charging stations

Table 3 Multiple linear regression results of the influence of interest points

POI	Regression coefficient	*p* value
Transportation facilities	6.35	0.022*
Commercial zone	4.37	0.032*
Official zone	2.72	0.047*
Residential zone	-8.64	0.009**
Recreation	2.48	0.015*

The results of the multiple linear regression with point of interest as a variable show that transportation facilities, such as train stations, bus stations, and subway stations, lead to an increase in the load of nearby charging stations. Commercial areas lead to a smaller increase in the load of nearby charging stations. Office areas likewise increase the load on nearby charging stations to some extent, especially during peak commuting hours. Residential areas may have relatively low loads on nearby charging stations, and recreational areas, such as movie theatres, parks, and restaurants, can lead to an increase in loads on nearby charging stations, especially during legal holidays. As a third pattern, there is also a relationship between charging stations that are farther apart where loads affect each other, mainly due to user behaviour. This is because user charging needs migrate to more distant areas with their individual driving behaviour. Therefore, the spatial dependency of long distances should also be considered.

3.4 Models construction

The objective of this paper is to predict the spatial distribution of charging loads at the target time X_{t+1} based on the historical data $\{ X_t \mid t = 0,1,\cdots,n-1 \}$ of the spatial and temporal distribution of electric vehicle electric loads within a single city. Each time period is a matrix containing the load values of all EV charging stations for the current time period. The relative position of each charging station is also reflected in the number of rows and columns of each value in the matrix.

On top of the historical data on the spatial and temporal distribution of loads, the influence of multiple sources of factors is also considered and their information is introduced into the prediction model, including relevant road network characteristics, point-of-interest characteristics, legal holidays, and weather characteristics.

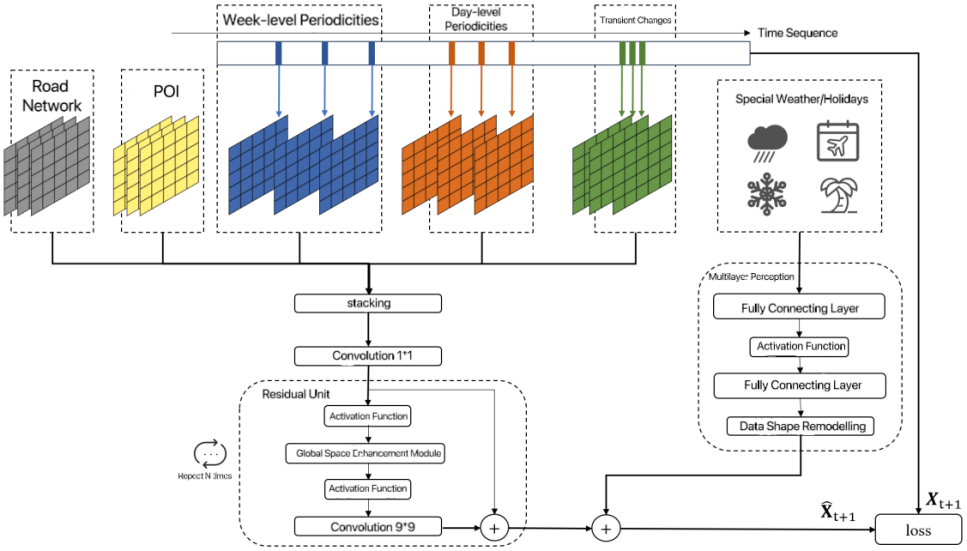

Fig. 9 Model framework

Fig. 9 shows the model architecture developed in this paper. The architecture consists of 4 parts, which are historical feature inputs, residual structure, global spatial enhancement module, and multi-layer perceptron with the introduction of time vectors. In a single round of model training, weekly-level periodicity, daily-level periodicity, short-term variations, road network information, and point-of-interest data from the historical dataset must be stacked together. A convolution operation is then performed to reduce the number of channels in the feature map through channel fusion, while keeping the feature map size unchanged. This operation aims to reduce the network's parameters and computational complexity while maintaining its performance. The result of the convolution operation is fed into the residual neural network, which undergoes an activation function, a global spatial reinforcement module, a second activation function, and this convolution operation to produce a final output of the matrix with the number of channels as one. At the same time, information about rainy days, snowy days, legal holidays, and other special times is input into the multi-layer perceptron in the form of vectors. The perceptron outputs a matrix with the same structure as the residual structure output matrix. These matrices are fused to produce the predicted value. The predicted value is then evaluated using a loss function to calculate the loss value for the current round of training. This loss value quantifies the degree of fit between the predicted value and the true value. Finally, the backpropagation method is used to calculate the gradient of the loss value, enabling the weights and biases of the network to be updated accordingly.

The historical characteristics of the inputs in the model include time-varying and stationary characteristics. The temporal variation characteristics change with the forecast target time change, and it includes weekly periodic information, daily periodic information and short time variation information, the support for introducing this information comes from the temporal characterization in Section 3.2 of this paper, and their model equations are as follows:

$$X_i^w = \left[X_{i-l_w}, X_{i-(l_w-1)}, \cdots, X_{i-w}\right] \tag{2}$$

$$X_i^d = \left[X_{i-l_d}, X_{i-(l_d-1)}, \cdots, X_{i-d}\right] \tag{3}$$

$$X_i^h = \left[X_{i-l_h}, X_{i-(l_h-1)}, \cdots, X_{i-1}\right] \tag{4}$$

It is assumed that the length of the selected time period is 1 hour (a = 24 hours). The week-level periodicity information X_i^w represents the information about the spatial distribution of the

charging station loadings on the same day and at the same hour in the same week w weeks prior to the target time i that needs to be predicted. For example, if the target time to be predicted is 17:00 on March 15, 2021 (Monday), the information of X_i^w is the spatial distribution matrix of charging station loads at 17:00 on March 8, March 1, and so on for the previous w Mondays. The day-level periodicity information X_i^d represents the information on the spatial distribution of the charging station loadings at the same hour on the d previous day i to the target time to be forecasted. For example, if the target time to be predicted is 17:00 on March 15, 2021, the information of X_i^d is the spatial distribution matrix of charging station loadings at 17:00 on March 14 at 17:00, March 13 at 17:00, and so on for the previous d days. The short time variation information X_i^h represents the spatial distribution information of the charging station loadings for the h hours before the target time i to be predicted. For example, if the target time to be predicted is March 15, 2021 at 17:00, the information of X_i^h is the spatial distribution matrix of charging station loadings for the h hours before March 15 at 16:00, March 15 at 15:00, etc.

Fixed features, on the other hand, do not change with the predicted target time. It includes point of interest and road network information. The support for introducing this information comes from the spatial characterization in 3.3. The equations are as follows:

$$X^{road} = [X_{A1}, X_{A2}, X_{B1}, X_{B2}, X_{C1}, X_{C2}] \tag{5}$$

$$X^{POI} = [X_{Trans}, X_{Busi}, X_{Admin}, X_{Residen}, X_{Enter}] \tag{6}$$

X_{road}consists of 6 layers of matrix stacking. Each layer represents the spatial distribution information of different types of roads. The corner symbols in the Eq. 5 are explained as follows.

$A1$ Unidirectional road of fast road type
$A2$ Bidirectional road of fast road type
$B1$ Unidirectional road of medium-speed road type
$B2$ Bidirectional road of medium-speed road type
$C1$ Unidirectional road of slow road type
$C2$ Bidirectional road of slow road type

X^{POI} consists of a stack of 5 layers of matrices, with each layer representing the spatial distribution information of different types of points of interest. The corner symbols in the equation are explained as follows.

$Trans$ Transportation facilities
$Busi$ Commercial area
$Admin$ Official area
$Residen$ Residential area
$Enter$ Recreational area

The rationale for introducing this information is that points of interest can have varying degrees of impact on the charging station loadings in their neighbourhoods. The charging station load prediction model built in this paper will stack the data mentioned above and feed it together into a convolutional layer. It is hoped that the model will establish connections between different times in this way as a way of extracting time-dependent information from the data.

A residual neural network is a framework for deep convolutional neural networks. The core idea of residual neural networks is to introduce residual connections into the model. These residual connections make it easier for the network to learn by skipping certain layers and passing information directly. Specifically, assuming that the input to a certain layer is X. It is desired that the model learns a mapping of $F(X)$. In the residual module, the mapping is actually learned as $F(X) - X$,which is the residual mapping. After that the input X needs to be added with the residual mapping to get the final output$F(X) = F(X) - X + X$. This process can be represented by the following equation:

$$output = F(X) + X \tag{7}$$

Compared to traditional convolutional neural networks, this jump connection makes it easier for gradients to circulate during back-propagation, thus alleviating the problems of gradient vanishing and gradient explosion, and allowing the network to be trained deeper as well as more easily. In the study of this paper, the residual unit that performs a single loop can be expressed as:

$$y = F(x, \{W\}) + x \tag{8}$$

where x represents input, y is output, $F(x, \{W\})$ is a function with a set of weights $\{W\}$. It represents a series of convolutional layers and activation functions. The result of the computation $F(x, \{W\})$ is added to the input x to get the output y. In a practical implementation, two or more convolutional layers may be included in $F(x, \{W\})$, as shown below:

$$F(x, \{W1, W2\}) = W2 * ReLU(W1 * x) \tag{9}$$

Here, $W1$ and $W2$ are the weights of the convolutional layers. $ReLU$ is the nonlinear activation function chosen for this model. Substituting this equation into the residual unit equation gives the final:

$$y = W2 * ReLU(W1 * x) + x \tag{10}$$

As shown in Fig. 10, the global spatial enhancement module we have created can extract the spatial dependency relationships at long distances within the network structure. The global spatial enhancement module first separates a portion of the channels from the regular convolution. These channels undergo global average pooling to reduce the number of parameters before entering the fully connected layer. The fully connected layer is designed to capture the long-range spatial dependency patterns between each pair of charging stations. Its output is added to the synchronous convolution output to provide the global spatial dependency parameters learned from the convolution output. This approach ensures that the global spatial enhancement module can output data of the same shape as the output of the regular convolution operation and can be used as input for the residual unit in the next loop.

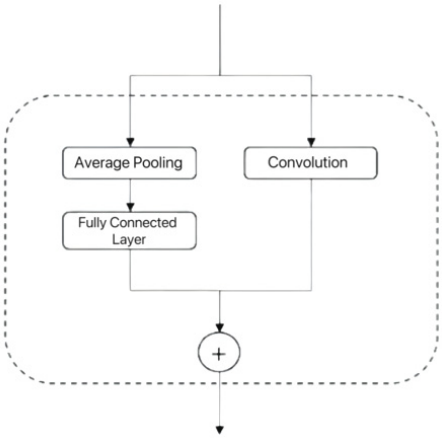

Fig. 10 Global space enhancement module

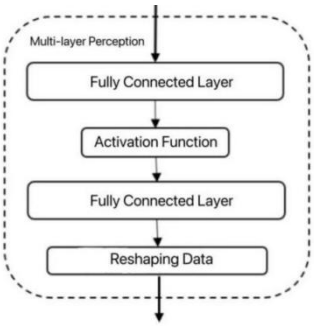

Fig. 11 Multi-layer percepton

In this model, the medium for learning special fixed-time features such as rainy or snowy weather and statutory holidays is a time vector introduced into the entire model through a multi-layer perceptron.

The time vector in the model is a vector of length $\alpha + 7 + 12 + 1 + 2$, where each component takes on the value of 0 or 1. The vector encodes the month to which the predicted target time belongs, the day of the week, the time interval within a day, whether it is a statutory holiday, and whether there is rainy or snowy weather on that day. Among them, the part of the time vector with a length of α encodes all time intervals within a day. If 1 hour is chosen as the time interval, then $\alpha = 24$. The part with a fixed length of 7 encodes the 7 days of the week. The part with a fixed length of 12 encodes the 12 months of the year. The part with a length of 1 indicates whether it is a statutory holiday. The part with a length of 2 indicates two types of weather found in the data that have a significant impact on the spatial-temporal distribution of the load.

The data format of the time vector is not a grid-like data graph that is passed between the structures of the model, so convolutional neural networks cannot be directly used to extract information from it. Therefore, a multi-layer perceptron is used here to learn the vector data and transform it into the same data shape as the output of other parts of the model.

A multi-layer perceptron is a type of feed-forward neural network where each layer is fully connected, enabling it to learn complex relationships between input features. In this model, the structure of the multi-layer perceptron is shown in Fig. 11. The time vector inputted is first dimensionally increased in the first fully connected layer, then goes through an activation function to enhance the model's non-linear expressive power. It then goes through additional fully connected layers to reach the desired data dimension $H \times W$, which is the matrix shape used for extracting the spatial distribution features of the charging stations in this study. Finally, after reshaping the data shape, it matches the output of the residual unit, and the two are added together to generate the prediction data.

4. Result and discussion

4.1 Modelling effectiveness evaluation

The evaluation metrics used in this study include Root Mean Square Error *(RMSE)* and the previously mentioned *MAE*. *RMSE* and *MAE* directly assess the error between predicted values and true values, facilitating an objective observation of the magnitude of deviations. Here, $X_i$represents the true value, and $\hat{X}_i$ represents the predicted value. The specific equation for RMSE is as follows:

$$RMSE = \sqrt{\frac{1}{T}\sum_{i=1}^{T} \|X_i - \hat{X}_i\|_2^2} \tag{11}$$

Consistent with the loss function, X_i and $\hat{X}_i$ represent the actual data and predicted data for the i^{th}time interval, respectively. T is the total number of samples in the test data.

After four-stages ablation experiments, as shown in Table 4, the smaller the value of the evaluation metric, the smaller the deviation between the predicted values and the actual values, indicating a better model performance. It can be observed from the evaluation metric data that gradually introducing the global spatial enhancement module, road network and point-of-interest information, legal holidays, and special weather information into the model leads to a gradual improvement in the overall model effectiveness. This demonstrates that incrementally adding new components to the model during its construction can optimize the accuracy of the model predictions.

Table 4 Results of ablation experiment

Modelling stage	RMSE	MAE
Base model	5.87	3.54
Base model + global space enhancement module	5.49	3.41
Base model + global spatial enhancement module + road network & points of interest	5.34	3.32
Full model	5.27	3.28

Table 5 presents the performance of the model constructed in this study compared to other baseline models in terms of evaluation metrics. It also compares the performance of models with different parameters. The parameter selection for the number of time periods within a day is set to 24 hours, representing the division of a day into 24 time periods, each lasting 1 hour. The parameter selection of 48 hours represents dividing a day into 48 time periods, each lasting 30 minutes. The best performance in terms of evaluation metrics is highlighted in bold in the table.

In the evaluation results, it was observed that the performance of various models with a time period length of 30 minutes was better than the performance with a time period length of 1 hour. Additionally, the model proposed in this paper outperformed the best-performing baseline model, which was a Residual Neural Network model, in two evaluation metrics. When compared to the Residual Neural Network model, the proposed model achieved a 10.2 % decrease in *RMSE* and a 7.3 % decrease in *MAE*. This indicates that the proposed model exhibits good performance in predicting the spatial-temporal distribution of electric vehicle charging station loads.

Table 5 Baseline model comparison results

Model	1 hour		30 minutes	
	RMSE	*MAE*	*RMSE*	*MAE*
Historical Average Model	10.17	6.59	9.24	6.02
Auto-regressive Integrated Moving Average Model (ARIMA)	9.88	6.51	8.19	5.69
Recurrent Neural Network (RNN)	9.12	5.86	6.97	4.28
Long Short-Term Memory Network (LSTM)	8.79	5.83	6.81	4.13
Convolutional Long Short-Term Memory Network (ConvLSTM)	7.32	4.22	6.02	3.85
Graph Convolutional Neural Network (GCN)	7.87	4.28	6.23	3.99
Residual Neural Network (ResNet)	7.05	4.02	5.87	3.54
The model proposed in this paper	6.35	3.71	5.27	3.28

4.2 Predictive results analysis

In this section, to demonstrate the predictive effectiveness of the model in real-world applications, the predictive results of the model are visualized. In the specific process, two charging stations are randomly selected from the dataset, and the actual load variations from Monday to Friday within a single week are extracted. The real data variations are then compared with the predicted data variations. The comparisons are illustrated in Figs. 12 and 13.

From the comparison between the predicted values and the actual values, it can be seen that the spatiotemporal load forecasting model in this paper can accurately predict the trends and magnitudes of load variations for each charging station. While the model successfully predicts the general trends of load increase and decrease for the majority of cases, there are discrepancies in predicting the specific numerical values of load peaks and valleys, especially in complex and variable real-world scenarios. Overall, the predictive performance of the model is in line with expectations.

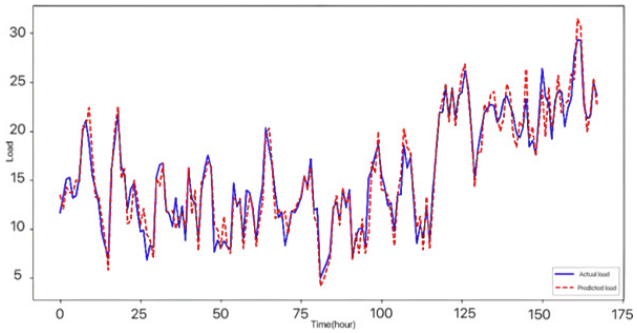

Fig. 12 Comparison between predicted and actual load values of a charging station A

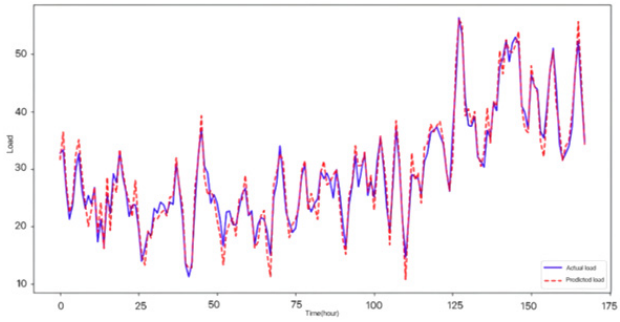

Fig. 13 Comparison between the predicted and actual load values of a charging station B

4.3 Parameter impact analysis

In the global spatial enhancement module, to capture long-distance spatial dependencies, some channels of the convolutional neural network are allocated to the fully connected layer. The role of the fully connected layer is to learn global spatial information. Fig. 14 illustrates the impact of the number of channels allocated to the fully connected layer on the model's predictive performance while keeping the total number of channels constant at 128. The graph shows that as the number of channels allocated to the fully connected layer increases from 0 to 1, the model immediately benefits, indicating that learning long-distance spatial dependencies in the dataset is meaningful for prediction. The model performs better with 24 separate channels, but performance decreases with more separate channels. This suggests that both short-distance spatial dependencies and long-distance spatial dependencies are significant and cannot be ignored.

The impact of the total number of channels in the convolutional neural network on the prediction results is shown in Fig. 15. The evaluation covers a range of total channels from 16 to 128. The results indicate that as the number of channels increases, the computational cost also increases, and the model's predictive performance benefits from the increase in the number of channels. However, the rate of improvement decreases gradually with the increase in the number of channels. An increase in the total number of channels leads to diminishing returns in the model's predictive performance. Therefore, we clearly defined the predictive goals for the spatiotemporal distribution of electric vehicle charging station loads and proposed a multi-feature fusion prediction model based on residual neural networks. This model learns the short-term variations, multi-periodicity, long-term trends, and special time influences of electric vehicle charging station loads in the time dimension. In the spatial dimension, it integrates road network information, charging station location information, and various points of interest locations, enabling the model to learn the spatial distribution patterns of electric vehicle charging station loads. Additionally, spatial dependencies are categorized into short-distance and long-distance categories, and a global spatial enhancement module is designed to help the model focus on long-distance spatial dependencies while retaining some channels for learning short-distance spatial dependencies.

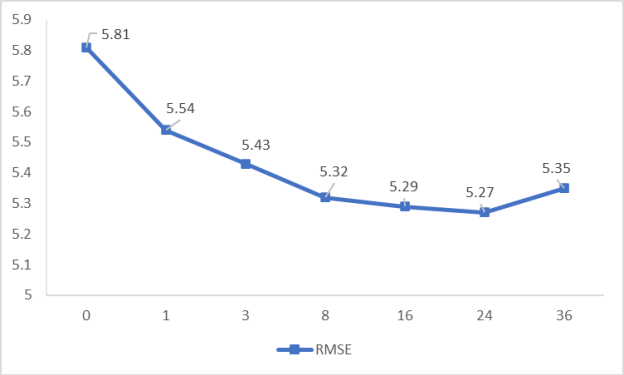

Fig. 14 The effect of the number of channels in the full connection layer on the results

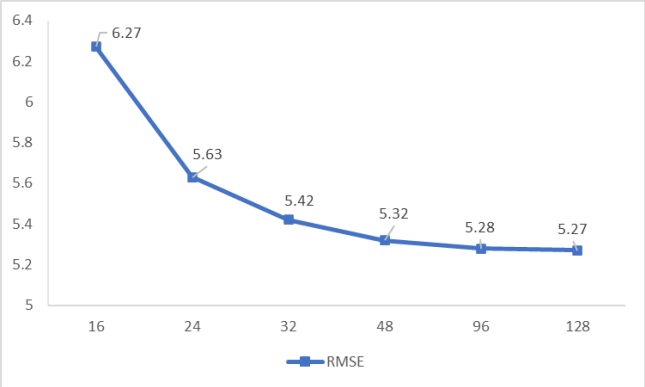

Fig. 15 Influence of amount of all channels

In the training process, the loss function *MSE* and relevant parameters in the model are defined. During the model evaluation phase, *RMSE* and *MAE* are used as evaluation metrics, and ablation experiments and comparative experiments are conducted. Ablation experiments involve gradually adding key components to observe the prediction errors, showing that the introduction of each component significantly enhances the model's predictive performance. In comparative experiments, the proposed model's superior performance in predicting the spatio-temporal distribution of electric vehicle charging station loads is demonstrated by comparing *RMSE* and *MAE* metrics, with reductions of 10.2 % and 7.3 %, respectively, compared to existing baseline models in the field.

4.4 User demand analysis

To avoid queuing at congested charging stations, users currently rely on real-time information provided by charging station operation platforms and map-based navigation applications to determine which charging stations still have available spaces. However, the rapid fluctuations in the load and availability of charging stations make the information on the saturation status of charging stations outdated by the time users arrive at the station or during their journey. This lag in information may lead to discrepancies between users' expectations and the actual situation when making charging station selection decisions based on outdated information, such as arriving at a station only to find it fully occupied, necessitating a waiting queue. User decisions on charging station selection heavily rely on the saturation status information of charging stations, but the uncertainty stemming from the time lag in this information has become a major pain point in the chain of electric vehicle charging behaviour for users.

Currently, the pain point primarily lies in the fact that electric vehicle users need to plan their charging station selections along the route in advance before embarking on long-distance drives. However, since the arrival times at each charging station along the long-distance route vary, the pre-queried saturation status information of charging stations also varies in terms of time lag based on the different arrival times. Due to the varying time lag of the real-time saturation status information that users rely on, planning a rational strategy for selecting multiple charging stations before a long-distance journey becomes challenging. This strategy requires accurate prediction of the saturation status information at multiple charging stations in the future, serving as deterministic information to support decision-making.

4.5 Charging station selection strategy support

The electric vehicle charging station load spatial-temporal prediction model established in this paper can output predicted values of load levels at multiple charging stations across various time intervals and locations in the future. By combining the predicted load data with the actual saturation levels of the charging stations, it is possible to determine which stations will experience queue congestion or excessive idleness at specific times in the future. In a specific process, defining the saturation load level of a particular electric vehicle charging station as L_{max} and the predicted load level at a future time as L_i, queue congestion coefficient as α, and idleness coefficient as β, where $\alpha > \beta$. Based on the comparison between the load levels L_{max} and L_i of a charging station

at a specific time in the future, the load saturation status of any charging station at any time and location in the future can be defined. The load saturation status can be categorized into the following three states:

Queue Congestion State (C): $L_i \geq \alpha * L_{max}$
Excessive Idle State (L): $L_i \leq \beta * L_{max}$
Normal Load State (N): $\beta * L_{max} < L_i < \alpha * L_{max}$

Based on the three divisions of load saturation states, the distribution of load saturation states for various charging stations at multiple future time points can be obtained. The schematic diagram of the load saturation states of each charging station in Shanghai at a single time point is shown in Fig. 16.

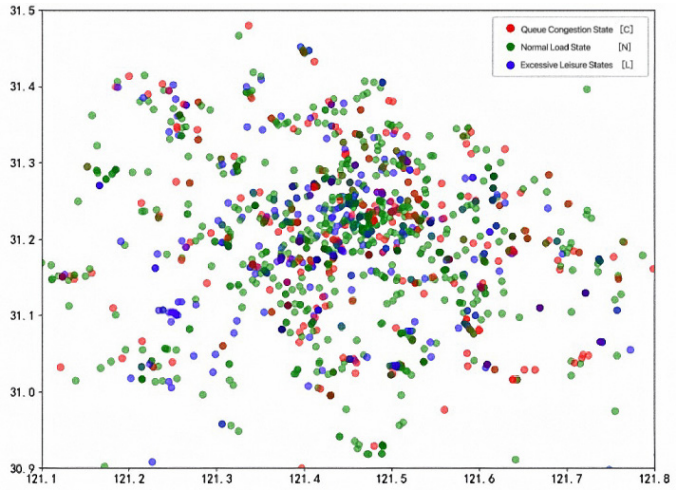

Fig. 16 Influence of amount of all channels

5. Conclusion and outlook

On this paper, the load capacity prediction model helps users to predict the load saturation state of charging stations at different locations within a certain range at different times. To help users identify charging stations where queuing is expected to occur at the target time for circumvention, it also helps users to identify charging stations with a large number of idle charging posts at the target time to minimize the risk of congestion. This provides users with relatively more accurate real-time predictive information for both one-time temporary charging station selection decisions and long-term charging plan development. However, the prediction model in this study mainly focuses on spatial and temporal distribution characteristics, and in the future, we can consider integrating more dimensions of information such as user behaviour and driving behaviour to improve the model's generalization ability and practicality.

Acknowledgments

This work was supported by the [National Natural Science Foundation of China] under Grant [62276020], [Beijing Natural Science Foundation] under Grant [9222025]. We appreciate their support very much.

References

[1] Chen, L.D., Zhang, Y., Figueiredo, A. (2019). A review of electric vehicle charging and discharging load forecasting research, *Automation of Electric Power Systems,* Vol. 43, No. 10, 177-197, doi: 10.7500/AEPS20180814001.
[2] Production and sales of major new energy vehicle enterprises in December 2020, *Automobile and Accessories* (2021), No. 2, 19.
[3] Liu, H., Yan, J., Ge, S.Y., Han, J. (2020). Dynamic response of electric vehicle and fast charging station considering the influence of multi-vehicle interaction, *Proceedings of the CSEE,* Vol. 40, No. 20, 6455-6468, doi: 10.13334/j.0258-8013.pcsee.191612.

[4] Liu, J.-Y., Liu, S.-F., Gong, D.-Q. (2021). Electric vehicle charging station layout based on particle swarm simulation, *International Journal of Simulation Modelling*, Vol. 20, No. 4, 754-765, doi: 10.2507/IJSIMM20-4-CO17.
[5] Ren, Q.L., Liu, H., Xiong, W. (2015). Introduction to the development of electric vehicle, *Power Supply Technologies and Application*, Vol. 18, No. 5, 10-16.
[6] Wang, Y., Shi, J., Wang, R., Liu, Z., Wang, L. (2018). Siting and sizing of fast charging stations in highway network with budget constraint, *Applied Energy*, Vol. 228, No. 17, 1255-1271, doi: 10.1016/j.apenergy.2018.07.025.
[7] Li, H., Yu, L., Chen, Y., Tu, H., Zhang, J. (2023). Uncertainty of available range in explaining the charging choice behavior of BEV users, *Transportation Research Part A: Policy and Practice*, Vol. 170, Article No. 103624, doi: 10.1016/j.tra.2023.103624.
[8] Daina, N., Polak, J.W., Sivakumar, A. (2015). Patent and latent predictors of electric vehicle charging behavior, *Transportation Research Record*, Vol. 2502, No.1, 116-123, doi: 10.3141/2502-14.
[9] Yang, Y., Yao, E., Yang, Z., Zhang, R. (2016). Modeling the charging and route choice behavior of BEV drivers, *Transportation Research Part C: Emerging Technologies*, Vol. 65, 190-204, doi: 10.1016/j.trc.2015.09.008.
[10] Latinopoulos, C., Sivakumar, A., Polak, J.W. (2017). Response of electric vehicle drivers to dynamic pricing of parking and charging services: Risky choice in early reservations, *Transportation Research Part C: Emerging Technologies*, Vol. 80, 175-189, doi: 10.1016/j.trc.2017.04.008.
[11] Al-Kandari, A.M., Soliman, S.A., El-Hawary, M.E. (2003). Fuzzy systems application to electric short-term load forecasting: Part II - Computational results, In: *Proceedings of Large Engineering Systems Conference on Power Engineering,* Montreal, Canada,131-137, doi: 10.1109/LESCPE.2003.1204692.
[12] Aliakbari Sani, S., Bahn, O., Delage, E., Tchuendom, R.F. (2022). Robust integration of electric vehicles charging load in smart grid's capacity expansion planning, *Dynamic Games and Applications*, Vol. 12, No. 3, 1010-1041, doi: 10.1007/s13235-022-00454-y.
[13] Huang, N., He, Q., Qi, J., Hu, Q., Wang, R., Cai, G., Yang, D. (2022). Multinodes interval electric vehicle day-ahead charging load forecasting based on joint adversarial generation, *International Journal of Electrical Power & Energy Systems*, Vol. 143, Article No. 108404, doi: 10.1016/j.ijepes.2022.108404.
[14] Liu, K., Liu, Y. (2023). Stochastic user equilibrium based spatial-temporal distribution prediction of electric vehicle charging load, *Applied Energy*, Vol. 339, Article No. 120943, doi: 10.1016/j.apenergy.2023.120943.
[15] Wang, D.L., Ding, A., Chen, G.L., Zhang, L. (2023). A combined genetic algorithm and A* search algorithm for the electric vehicle routing problem with time windows, *Advances in Production Engineering & Management*, Vol. 18, No. 4, 403-416, doi: 10.14743/apem2023.4.481.
[16] Bian, H., Zhou, C., Guo, Z., Wang, X., He, Y., Peng, S. (2022). Planning of electric vehicle fast-charging station based on POI interest point division, functional area, and multiple temporal and spatial characteristics, *Energy Reports*, Vol. 8, Supplement 15, 831-840, doi: 10.1016/j.egyr.2022.10.161.
[17] Zhang, K., Tian, Y., Shi, S., Su, Y., Xu, L., Zhang, M. (2021). Electric vehicle charging demand forecasting based on city grid attribute classification, In: *Proceedings of 2021 11th International Conference on Power and Energy Systems (ICPES),* Shanghai, China, 592-597, doi: 10.1109/ICPES53652.2021.9683949.
[18] Bayram, I.S., Galloway, S. (2022). Pricing-based distributed control of fast EV charging stations operating under cold weather, *IEEE Transactions on Transportation Electrification*, Vol. 8, No. 2, 2618-2628, doi: 10.1109/TTE.2021.3135788.
[19] Louie, H.M. (2017). Time-series modeling of aggregated electric vehicle charging station load, *Electric Power Components and Systems*, Vol. 45, No. 14, 1498-1511, doi: 10.1080/15325008.2017.1336583.
[20] Bampos, Z.N., Laitsos, V.M., Afentoulis, K.D., Vagropoulos, S.I., Biskas, P.N. (2024). Electric vehicles load forecasting for day-ahead market participation using machine and deep learning methods, *Applied Energy*, Vol. 360, Article No. 122801, doi: 10.1016/j.apenergy.2024.122801.
[21] Huang, Y., Kockelman, K.M. (2020). Electric vehicle charging station locations: Elastic demand, station congestion, and network equilibrium, *Transportation Research Part D: Transport and Environment*, Vol. 78, Article No. 102179, doi: 10.1016/j.trd.2019.11.008.
[22] Unterluggauer, T., Rauma, K., Järventausta, P., Rehtanz, C. (2021). Short-term load forecasting at electric vehicle charging sites using a multivariate multi-step long short-term memory: A case study from Finland, *IET Electrical Systems in Transportation*, Vol. 11, No. 4, 405-419, doi: 10.1049/els2.12028.